BRAIN CONNECTIVITY
Volume 5, Number 5, 2015

DOI: 10.1089/brain.2014.0304

Brain Graph Topology Changes Associated with Anti-Epileptic Drug Use

Zulfi Haneef,[1,2,*] Harvey S. Levin,[3] and Sharon Chiang[4,*]

Abstract

Neuroimaging studies of functional connectivity using graph theory have furthered our understanding of the network structure in temporal lobe epilepsy (TLE). Brain network effects of anti-epileptic drugs could influence such studies, but have not been systematically studied. Resting-state functional MRI was analyzed in 25 patients with TLE using graph theory analysis. Patients were divided into two groups based on anti-epileptic medication use: those taking carbamazepine/oxcarbazepine (CBZ/OXC) ($n=9$) and those not taking CBZ/OXC ($n=16$) as a part of their medication regimen. The following graph topology metrics were analyzed: global efficiency, betweenness centrality (BC), clustering coefficient, and small-world index. Multiple linear regression was used to examine the association of CBZ/OXC with graph topology. The two groups did not differ from each other based on epilepsy characteristics. Use of CBZ/OXC was associated with a lower BC. Longer epilepsy duration was also associated with a lower BC. These findings can inform graph theory-based studies in patients with TLE. The changes observed are discussed in relation to the anti-epileptic mechanism of action and adverse effects of CBZ/OXC.

Key words: anti-epileptic drugs; betweenness centrality; carbamazepine; clustering coefficient; global efficiency; graph theory; small-world index; temporal lobe epilepsy

Introduction

EPILEPSY IS THOUGHT to be a network disease, and much research has focused on evaluating its effects on different brain networks. Research has found that focal epilepsies such as temporal lobe epilepsy (TLE) can affect different parts of the brain, including networks concerned with memory, behavior, thought, and sensory function (Pillai et al., 2007). Several studies have used functional MRI (fMRI) to study brain networks in TLE, many of which have used graph theory analysis methods (Chiang and Haneef, 2014). However, functional techniques can be confounded by the effects of anti-epileptic drugs, which are known to affect brain function.

Graph theory research is a technique that has recently been increasingly applied to the study of brain networks across several modalities, including structural/functional neuroimaging and neurophysiology (Chiang and Haneef, 2014). It has advantages in being especially sensitive to changes in brain network structure (Bullmore and Bassett, 2011), and may provide a useful method for studying the effect of anti-epileptic drugs on brain networks. This sensitivity may also make graph theory-based research particularly prone to confounds from anti-epileptic drug effects. Interpreting results of graph theoretic studies in epilepsy have been limited by the absence of literature documenting anti-epileptic drug effects (Chiang and Haneef, 2014; Horstmann et al., 2010). We undertook this study to understand the network effects of anti-epileptic drugs to understand the mechanisms of drug action and adverse effects, as well as to help interpret graph theory studies where the effect of anti-epileptic medications could be a potential confound.

In this study, we analyzed the association of the anti-epileptic medications carbamazepine and oxcarbazepine (CBZ/OXC) on graph theory-based network parameters (global efficiency [GE], betweenness centrality [BC], clustering coefficient, and small-world index) of functional connectivity (FC) MRI in patients with TLE to (1) assess

[1]Department of Neurology, Baylor College of Medicine, Houston, Texas.
[2]Neurology Care Line, VA Medical Center, Houston, Texas.
[3]Department of Physical Medicine, Baylor College of Medicine, Houston, Texas.
[4]Department of Statistics, Rice University, Houston, Texas.
*Both authors contributed equally to this work.

whether and how CBZ/OXC affects network parameters in TLE, and (2) determine the effects of demographic and epilepsy characteristics on network parameters.

Materials and Methods

Subjects and data collection

A total of 39 subjects (14 left TLE, 11 right TLE, and 14 controls) were recruited for the study after appropriate Institutional Review Board approvals, and informed consent was obtained. Patients were recruited from the Baylor College of Medicine comprehensive epilepsy center, and had lateralized TLE diagnosed by semiology, MRI, and video-EEG monitoring. Patients with significant cognitive impairment or the presence of major neurological/psychiatric co-morbidities (other than epilepsy) were excluded. Healthy control subjects, matched for age and sex, were included in the study only for the purposes of providing a standard reference for average levels of network topology. The study protocol conforms to the Helsinki Declaration of 1975, as revised in 2008.

Records were reviewed for age, sex, epilepsy duration, full-scale IQ, MRI findings, video EEG findings, and antiepileptic drug regimen, and are summarized in Table 1. Differences in network topology between patients on CBZ/OXC (+CBZ/OXC) as compared with patients not on CBZ/OXC (−CBZ/OXC) were computed. There were 9 patients in the +CBZ/OXC group (6 left TLE, 3 right TLE), and 16 patients in the −CBZ/OXC (8 left TLE, 8 right TLE) groups.

fMRI data acquisition

Neuroimaging was performed on a Philips Ingenia 3T scanner (Philips). T1 images were acquired using a three-dimensional inversion recovery prepared, segmented k-space gradient echo sequence as follows: 220 phase encoding steps; TR/TE = 8 msec/4.0 msec; flip angle = 8 degrees; time between successive TFE shots = 3000 msec; FOV = 240 × 220 × 170 mm^3; and acquired voxel size = 1 × 1 × 1 mm^3. Resting-state blood oxygenation level-dependent functional images were acquired as follows: TR = 6000 msec, TE = 30 msec, FOV = 228 mm, matrix = 100 × 100, slice thickness = 2.25 mm, 67 slices, and 100 volumes.

Head motion for the different subject groups were as follows: +CBZ/OXC (max rotation 0.61 degrees, max translation 0.85 mm, absolute displacement 0.47 mm, and relative displacement 0.24 mm); −CBZ/OXC (max rotation 0.55 degrees, max translation 0.66 mm, absolute displacement 0.26 mm, and relative displacement 0.17 mm). There was no significant difference between subject groups with regard to motion, including max rotation (Mann–Whitney U = 88, $p = 0.39$), max translation (Mann–Whitney U = 77, $p = 0.80$), absolute displacement (Mann–Whitney U = 86, $p = 0.45$), or relative displacement (Mann–Whitney U = 74, $p = 0.93$). Excessive head motion was controlled for using motion scrubbing (Power et al., 2012).

fMRI preprocessing

Preprocessing was performed using FSL (fMRIB Software Library) v5.0.2 (Oxford; www.fmrib.ox.ac.uk/fsl) (Jenkinson et al., 2012). The first 12 sec were discarded for magnetization equilibrium. Non-brain tissue elimination (Smith, 2002), slice-timing correction, spatial smoothing (Gaussian kernel 5 mm FWHM), and linear co-registration to the T1-weighted structural image were followed by the Montreal Neurological Imaging (MNI) template. Common preprocessing steps for resting-state fMRI were then applied, including temporal bandpass filtering ($0.01 < f < 0.08$ Hz) and removal of the following sources of spurious variance using linear regression: six motion parameters and their temporal derivatives, white matter signal, and ventricular signal (Fox et al., 2005). Whole-brain signal regression was not performed, to increase test-retest reliability in graph theory analyses (Liang et al., 2012). Motion scrubbing was performed (Power et al., 2012), and residuals were further normalized before analysis.

Graph construction and calculation of network graph theory metrics

After registration to the MNI template image, functional images were parcellated into 90 anatomical regions using the automated anatomical labeling atlas (Tzourio-Mazoyer et al., 2002). Representative time series for each region (averaged residual time series across all its voxels) were correlated to each other using Pearson's correlation coefficient. After setting negative correlations to zero, binary unweighted graphs were constructed by thresholding across the biologically plausible range of connection densities (Rubinov and Sporns, 2010), yielding a range of potential undirected brain functional network graphs. For each whole-brain graph, the following network graph theory measures were calculated and averaged across the non-random connection density range (Bullmore and Bassett, 2011).

Clustering coefficient (γ)

Clustering coefficient provides a measure of the level of ''cliquishness'' of a network (Bullmore and Bassett, 2011). Lower levels of clustering coefficient have been demonstrated to be associated with greater cognitive decline in TLE (Vlooswijk et al., 2011). Nodal clustering coefficient (C_i) was calculated as the ratio of the number of existing to possible connections in G_i, the subgraph of node i:

$$C_i = \frac{E_i}{K_i(K_i - 1)/2}$$

where E_i denotes the number of edges in subgraph G_i, and K_i denotes the degree of node i. The absolute clustering coefficient of the network (C) was then calculated as the average value of C_i over all nodes (Rubinov and Sporns, 2010). To avoid the influence of other network characteristics, γ was calculated as the ratio of C to C_{random}, the averaged clustering coefficient over 500 randomly rewired null models (Maslov and Sneppen, 2002):

$$\gamma = \frac{C}{C_{random}}.$$

Global efficiency

GE provides a measure of the ability of the network to transmit information at a global level (Latora and Marchiori, 2001, 2003). Nodal efficiency was calculated as the mean of the inverse shortest path lengths from a given node to all

other nodes. GE was then calculated as the average nodal efficiency over all nodes:

$$GE = \frac{1}{N(N-1)} \sum_{i \neq j \in G} \frac{1}{d_{ij}},$$

where d_{ij} is the shortest path length between nodes i and j in graph G, and N denotes the number of nodes.

Average BC

Average BC provides a measure of the ''hubness'' of a network. The BC of each node was calculated as the number of shortest paths in the network that pass through the given node, divided by the total number of shortest paths in the network:

$$BC_i = \sum_{m \neq i \neq n \in G} \frac{\sigma_{mn}(i)}{\sigma_{mn}}$$

where σ_{mn}denotes the total number of shortest paths from node m to n, and $\sigma_{mn}(i)$ denotes the number of shortest paths from m to n that pass through i. Nodes with high values of BC are located on highly traveled paths. Average BC was then calculated as the average BC over all nodes:

$$BC = \frac{1}{N} \sum_i BC_i.$$

Small-world index (σ)

Small-world index is a measure of the network's balance between segregation and integration, and was calculated as the ratio of clustering coefficient to characteristic path length:

$$\sigma = \frac{\gamma}{\lambda}$$

where λ is the characteristic path length.

These measures were chosen, as they are most frequently examined in graph theoretic studies of TLE. Graph theory metrics were calculated using the Brain Connectivity Toolbox (Rubinov and Sporns, 2010). MATLAB (MathWorks) was used for graph construction and topology calculations.

Statistical analysis

Statistical analyses were performed using R v3.0.1 (R Foundation).

Multiple linear regression was used to assess whether patients taking CBZ/OXC (+CBZ/OXC) had different levels of functional network topology (γ, GE, BC, σ) compared with patients without CBZ/OXC in their medication regimen (−CBZ/OXC), while controlling for baseline characteristics (age, sex, epilepsy duration, and drug load) as

Table 1. Baseline Characteristics and Anti-Epileptic Drug Daily Dosages for Unilateral Temporal Lobe Epilepsy Patients

Age (years)	*Gender*	*Epilepsy duration (years)*	*AED dose (mg/day)*	*MRI findings*	*VEEG*	*FSIQ score (percentile)*
			Left TLE			
33	F	16	CBZ 1000 mg, PHT 300 mg	L MTS	LT	83 (13%)
23	F	4	LTG 200 mg, PGB 50 mg	L MT fullness (CD/neoplasm)	LT	87 (19%)
22	F	4	LCM 200 mg, LTG 200 mg, TPM 175 mg	Normal	LT	82 (12%)
67	F	64	LEV 1000 mg	L MTS	LT	Not done
22	M	5	LEV 1000 mg, OXC 1200 mg	Normal	LT	86 (18%)
23	F	11	FBM 2400 mg, ZNS 400 mg	L MT fullness (CD/neoplasm)	LT	96 (39%)
39	F	27	LTG 600 mg, ZNS 200 mg, CBZ 200 mg	L MT hyperintensity	LT	Not done
32	M	17	CBZ 600 mg, LEV 3000 mg	Normal	LT	82 (12%)
38	F	6	LTG 450 mg, ZNS 300 mg	L MT hyperintensity	LT	98 (83%)
37	F	22	LTG 300 mg, CBZ 1200 mg, LCM 300 mg	Bilateral H hyperintensity	LT	Not done
42	F	9	LTG 500 mg	L MT CD	LT	Not done
33	F	12	LTG 200 mg, LEV 1500 mg, AZ 500 mg	L MT CD	LT	103 (58%)
28	M	2	LEV 3000 mg, OXC 600 mg	Normal	LT	91 (27%)
53	F	7	LTG 400 mg	L MT fullness	LT	97 (42%)
			Right TLE			
47	F	3	LCM 400 mg	R MTS	RT	96 (39%)
36	M	30	LTG 600 mg, ZNS 300 daily	Mild generalized volume loss	RT	Not done
21	M	9	LCM 300 mg, PHT 400 mg	Normal	RT	Not done
28	M	6	LEV 750 mg, LTG 200 mg, TPM 50 mg	R H fullness/hyperintensity	RT	77 (6%)
57	M	5	VPA 200 mg, OXC 2400 mg	R MTS	RT	89 (23%)
37	M	27	LTG 400 mg, CBZ 600 mg	R cavernous malformation	RT	99 (47%)
49	F	48	LEV 1500 mg, LCM 450 mg, RUF 800 mg	R MT hyperintensity/atrophy, L MT hyperintensity	RT	92 (30%)
38	F	32	LEV 1000 mg, LTG 200 mg	R MTS	RT	94 (34%)
61	F	56	LTG 300 mg, PHT 300 mg, VPA 750 mg	R MTS	RT	66 (1%)
56	M	56	LEV 3000 mg, VPA 1000 mg	R H atrophy	RT	63 (1%)
43	F	39	CBZ 1000 mg, LCM 400 mg	R H atrophy/hyperintensity	RT	87 (19%)

AED, anti-epileptic drug; AZ, acetazolamide; BT, bilateral temporal; CBZ, carbamazepine; CD, cortical dysplasia; F, female; FBM, felbamate; FSIQ, full-scale IQ; H, hippocampus; L, left; LCM, lacosamide; LEV, levetiracetam; LT, left temporal; LTG, lamotrigine; M, male; MT, mesial temporal; MTS, mesial temporal sclerosis; NL, not lateralized; OXC, oxcarbazepine; PGB pregabalin; PHT, phenytoin; TLE, temporal lobe epilepsy; R, right; RT, right temporal; TPM, topiramate; VEEG, video electroencephalography; VPA, valproic acid; ZNS, zonisamide.

Table 2. Baseline Characteristics of Study Subjects

	+CBZ/OXC *n = 9*	*−CBZ/OXC* *n = 16*	*HC* *n = 14*	p-*Value*
Age	36.4 ± 9.9	39.8 ± 14.6	35.4 ± 8.0	0.49[a]
Male (vs. female)	5 (4)	4 (12)	7 (7)	0.20[b]
FSIQ percentile	22.7 ± 11.9	30.3 ± 24.5	—	0.49[a]
Left TLE (vs. right TLE)	6 (3)	8 (8)	—	0.68[b]
Epilepsy duration (years)	17.8 ± 12.3	22.3 ± 21.9	—	0.50[a]
Polytherapy (vs. monotherapy)	9 (0)	12 (4)	—	0.26[b]
Drug load	2.5 ± 1.1	2.4 ± 1.5	—	0.53[a]

Mean ± standard deviation are shown for continuous variables; counts are shown for categorical variables. *p*-values are for comparison of +CBZ/OXC with −CBZ/OXC study groups.
[a]Nonparametric permutation testing based on 1000 resamples.
[b]Fisher's exact test.
HC, healthy controls.

well as preexisting connectomic changes resulting from differences in TLE laterality. ANOVA *F* tests were first used to evaluate the omnibus hypothesis of at least one regression coefficient that was significantly different from zero. Drug load was calculated as the ratio of prescribed daily dose to defined daily dose (Supplementary Table S1; Supplementary Data are available online at www.liebertpub.com/brain), following earlier pharmaco-fMRI (Vaessen et al., 2012; Vlooswijk et al., 2010) and quantitative anti-epileptic drug studies (Lammers et al., 1995). To improve robustness of regression estimates, influential observations with a Cook's distance of greater than 4/n were excluded from analysis (Bollen and Jackman, 1990). Model fit was evaluated using standard residual analysis. Multicollinearity was assessed based on a variance inflation factor of greater than 10 (Hair Jr. et al., 1995).

Results

Table 1 shows the baseline demographic and disease-related characteristics, as well as the anti-epileptic drug dosages for the patient groups. Table 2 compares the +CBZ/

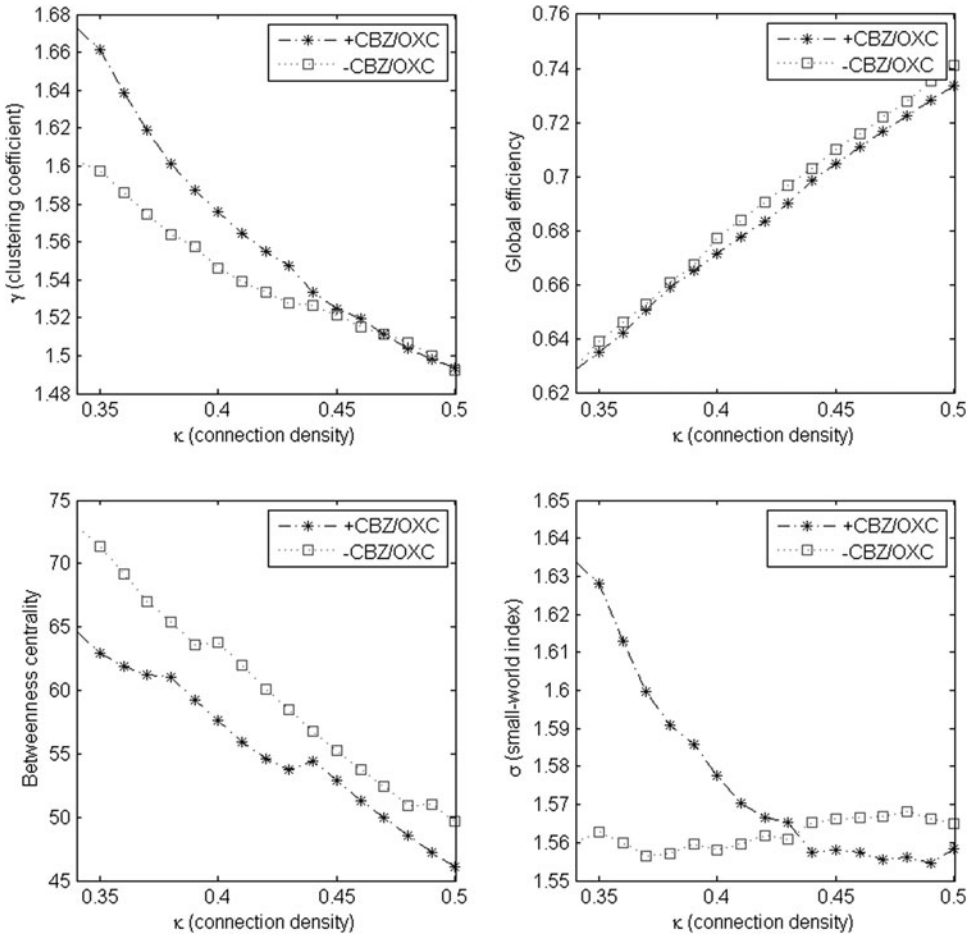

FIG. 1. Mean values of clustering coefficient (γ), global efficiency (GE), average betweenness centrality (BC), and small-world index (σ) across non-random connection density range (0.34–0.5).

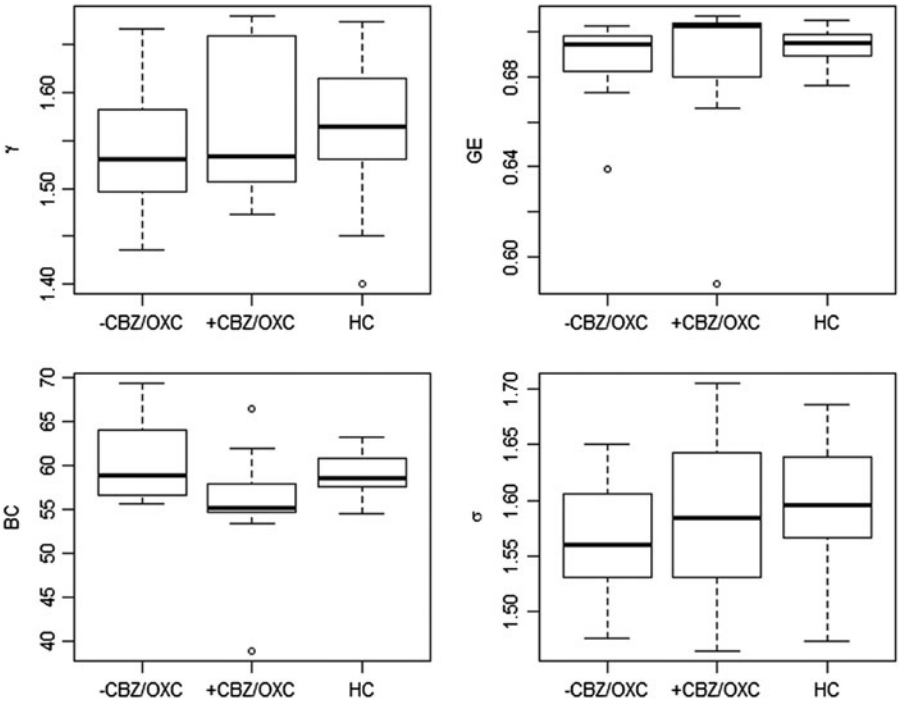

FIG. 2. Values of clustering coefficient (γ), GE, BC, and small-world index (σ) averaged across non-random connection density range. Levels of network topology for healthy controls are shown for reference. HC, healthy controls; GE, global efficiency; BC, betweenness centrality.

OXC and −CBZ/OXC with regard to baseline characteristics. +CBZ/OXC and −CBZ/OXC groups did not differ significantly with regard to age, gender, full-scale IQ score, TLE laterality, epilepsy duration, number of patients on poly- versus monotherapy, or drug load.

Figure 1 compares estimated levels of clustering coefficient, GE, average BC, and small-world index across different levels of the non-random connection density range. BC was consistently lower in +CBZ/OXC patients across the entire non-random connection density range. γ was higher in +CBZ/OXC patients in networks with lower connection densities, but similar to −CBZ/OXC patients in networks with higher connection densities. GE was similar in +CBZ/OXC and −CBZ/OXC patients across the entire non-random connection density range. σ was higher in +CBZ/OXC patients in networks with lower connection densities and higher in −CBZ/OXC patients in networks with higher connection densities (Fig. 1).

Figure 2 shows the mean levels of clustering coefficient, GE, average BC, and small-world index averaged across the non-random connection density range for +CBZ/OXC and −CBZ/OXC groups, with mean network topology levels of healthy controls provided for reference.

Multiple linear regression showed that the omnibus hypothesis was significant for BC ($F=3.697$, df = 6/15, $p=0.019$). +CBZ/OXC had a lower BC than −CBZ/OXC. Longer epilepsy duration was also associated with a lower network BC (Table 3). The omnibus hypothesis was not significant for GE ($F=1.379$, df = 6/16, $p=0.28$), γ ($F=1.11$, df = 6/15, $p=0.40$), or σ ($F=1.52$, df = 6/15, $p=0.24$; Supplementary Table S3). The mean BC difference for the various brain regions between the +CBZ/OXC and −CBZ/OXC groups is shown in Table 4, and shown as a color coded map in Figure 3. The mean BC difference for the various brain regions associated with duration of epilepsy is shown in Supplementary Table S2, and shown as a color-coded map in Supplementary Figure 1.

Discussion

We sought to study the association of anti-epileptic drugs with changes in brain network functional topology to aid

TABLE 3. MULTIPLE LINEAR REGRESSION OF BETWEENNESS CENTRALITY ON CBZ/OXC

	BC		
Covariate	*Coefficient (95% confidence interval)*	*P(>|t|)*	*VIF*
+CBZ/OXC	**−5.581 (−10.103, −1.059)**	**0.02**	**1.19**
Epilepsy duration (years)	**−0.164 (−0.314, −0.014)**	**0.03**	**2.04**
Gender	3.387 (−1.898, 8.673)	0.19	1.52
Age	0.192 (−0.037, 0.421)	0.09	2.25
TLE laterality (+RTLE)	−2.967 (−7.864, 1.929)	0.22	1.49
Drug load	0.454 (−1.313, 2.221)	0.59	1.29

Variables significantly associated with the dependent variable at the 0.05 level are highlighted in bold.
BC, betweenness centrality; RTLE, right temporal lobe epilepsy; VIF, variance inflation factor.

TABLE 4. MEAN BETWEENNESS CENTRALITY DIFFERENCE IN THE DIFFERENT BRAIN REGIONS IN THE +CBZ/OXC GROUP, COMPARED WITH −CBZ/OXC IN PATIENTS WITH TEMPORAL LOBE EPILEPSY

Region	Mean difference	Region	Mean difference
Amygdala L	1.3	Occipital Inf R	-14.6
Amygdala R	-17.1	Occipital Mid L	-23.1
Angular L	-0.1	Occipital Mid R	-6.4
Angular R	-46.8	Occipital Sup L	-24.2
Calcarine L	-4.6	Occipital Sup R	-8.9
Calcarine R	-4.6	Olfactory L	-44.5
Caudate L	23.4	Olfactory R	-10.5
Caudate R	3.7	Pallidum L	8.8
Cingulum Ant L	-50.5	Pallidum R	-2.7
Cingulum Ant R	-56.1	Paracentral Lobule L	-14.6
Cingulum Mid L	14.2	Paracentral Lobule R	-27.3
Cingulum Mid R	7.6	ParaHippocampal L	13.1
Cingulum Post L	16.9	ParaHippocampal R	-16.5
Cingulum Post R	-0.3	Parietal Inf L	30.8
Cuneus L	-21.5	Parietal Inf R	3.5
Cuneus R	-23.3	Parietal Sup L	-13.9
Frontal Inf Oper L	-24.1	Parietal Sup R	-23.8
Frontal Inf Oper R	9.3	Postcentral L	-5.1
Frontal Inf Orb L	-56.7	Postcentral R	13.7
Frontal Inf Orb R	-3.5	Precentral L	3.1
Frontal Inf Tri L	-33.6	Precentral R	31.8
Frontal Inf Tri R	2.8	Precuneus L	3.5
Frontal Med Orb L	-27.3	Precuneus R	13.3
Frontal Med Orb R	-6.0	Putamen L	-55.9
Frontal Mid L	5.0	Putamen R	6.1
Frontal Mid Orb L	3.4	Rectus L	-19.8
Frontal Mid Orb R	10.3	Rectus R	10.3
Frontal Mid R	3.4	Rolandic Oper L	-12.6
Frontal Sup L	11.5	Rolandic Oper R	-13.6
Frontal Sup Medial L	-9.2	Supp Motor Area L	16.5
Frontal Sup Medial R	-23.0	Supp Motor Area R	-5.4
Frontal Sup Orb L	-6.6	SupraMarginal L	17.5
Frontal Sup Orb R	14.9	SupraMarginal R	16.4
Frontal Sup R	3.0	Temporal Inf L	-8.7
Fusiform L	23.4	Temporal Inf R	6.2
Fusiform R	-1.5	Temporal Mid L	-0.2
Heschl L	25.0	Temporal Mid R	-4.0
Heschl R	-5.0	Temporal Pole Mid L	9.5
Hippocampus L	-22.6	Temporal Pole Mid R	-7.7
Hippocampus R	-37.3	Temporal Pole Sup L	-9.5
Insula L	-30.0	Temporal Pole Sup R	0.3
Insula R	29.7	Temporal Sup L	54.3
Lingual L	1.8	Temporal Sup R	37.0
Lingual R	2.3	Thalamus L	-19.5
Occipital Inf L	10.2	Thalamus R	-39.5

Areas with lower BC in the +CBZ/OXC group are to the left of the median in the data bars shown, and regions with higher BC are to the right.

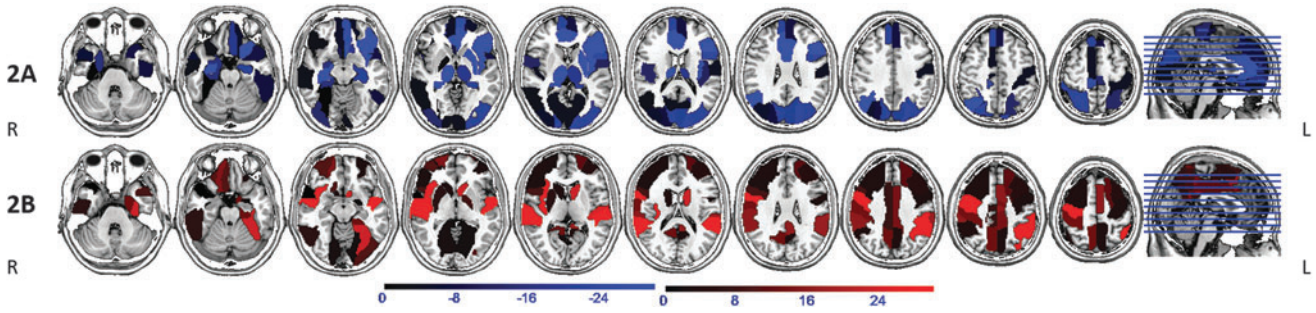

FIG. 3. Areas of reduced (2A, blue) and increased (2B, red) BC in patients on carbamazepine and oxcarbazepine (CBZ/OXC) compared with patients not on CBZ/OXC. Notable regions with BC reduction are seen in bilateral hippocampi, thalami, left insula, putamen, medial frontal and visual/sensori-motor cortex. BC increase is seen in right insula, caudate, fronto-parietal cortex, cingulum, and precuneus/retrosplenium. Orientation is radiological.

interpretability of graph theory-based connectivity studies in epilepsy, as well as to understand the mechanisms of drug action and adverse effects. Specifically, we looked at the effect of CBZ/OXC on graph theory metrics, finding that its use was associated with a lower BC in brain networks. In addition, we found that a longer epilepsy duration was also associated with a lower network BC. To our knowledge, effects of individual anti-epileptic drugs on graph theoretic measures of TLE brain networks have not been previously analyzed using graph theoretic methods.

BC indicates the presence of hyperconnected nodes that connect distant parts of the brain (hubs). Our findings suggest that CBZ/OXC treatment may influence hubness and consequently affect the network changes in epilepsy. In TLE, hubs have been noted to be redistributed from all cerebral lobes to the paralimbic and temporal association cortices (Bernhardt et al., 2011), and may include the epileptogenic zone (Wilke et al., 2011). We found widespread regions of BC reduction and increase with CBZ/OXC use. It is tempting to speculate that a redistribution of hubs within (and outside) the limbic circuit may lead to improved seizure control with CBZ/OXC use, and contribute to adverse effects. However, we do not have any direct evidence to prove that hypothesis. Within the limbic circuit thought to be involved in TLE, the hippocampal and thalamic BC were reduced with CBZ/OXC use, while cingulate and posterior cingulate/precuneus complex BC were increased. Our finding of reduced BC (hubness) in the hippocampi associated with CBZ/OXC use is in alignment with a previous pharmaco-fMRI study that found reduced activation of the hippocampi with the use of CBZ during a memory task (Jokeit et al., 2001). It is likely that the negative effects of anti-epileptic drugs may be mediated via reduction of hubness within the hippocampus.

Another group has previously examined the effect of anti-epileptic drug load on brain graph network metrics finding a negative association with clustering coefficient using diffusion tensor imaging (Vaessen et al., 2012), and a negative association with clustering coefficient and local efficiency using fcMRI (Vlooswijk et al., 2011). In these studies, it was inferred that a reduced clustering coefficient could be the mechanism mediating the association between reduced intellectual function and higher drug load (Vlooswijk et al., 2011). However, the effects of individual anti-epileptic drugs or anti-epileptic drug groups were not analyzed in these studies. An association between CBZ/OXC and either clustering coefficient or local efficiency was not detected in our study. Of note, our study groups were well matched based on drug load, which suggests that while drug load may exhibit a negative effect on clustering coefficient and local efficiency, usage of CBZ/OXC in the medication regimen does not.

We also found that, controlling for medication use, longer epilepsy duration was associated with a lower network BC (hubness), which may be related to the hub redistribution noted with TLE in earlier studies (Bernhardt et al., 2011; Chiang et al., 2014).

Limitations and future directions

One limitation of our study was a small sample size, which may have hidden some associations. The patients recruited were mostly on polytherapy. Although recruiting patients on monotherapy would be more straightforward to analyze, the effect of other anti-epileptic drugs and epilepsy-related factors was controlled for through regression analysis to avoid confounding results. Our use of +CBZ/OXC and −CBZ/OXC groups follows the example of previous pharmaco-fMRI studies (Jokeit et al., 2001; Szaflarski and Allendorfer, 2012). It has been noted that the effect of a drug on brain network properties would require repeat acquisitions in the same subject, on and off the drug being evaluated (Achard and Bullmore, 2007; Giessing and Thiel, 2012). Such an analysis cannot be performed using our current dataset, and could be a focus of future studies. A caveat to interpreting our results is that, although our results show an association of CBZ/OXC use with specific network changes, causation of these changes by the medication cannot be inferred.

Another limitation is the heterogeneity in etiologies of epilepsy, which may potentially cause varying effects on brain networks. However, all subjects had TLE confirmed by video EEG, and the rationale in considering them as a group was that they had similar seizures, which were thought to involve similar brain networks. Furthermore, we did not evaluate for an association between seizure control and network changes. Future studies should investigate whether particular network changes are associated with better seizure control, which would be a potential neuroimaging biomarker to predict response anti-epileptic use in patients with epilepsy.

A general limitation of resting-state fMRI studies is their potential to be contaminated by motion artifacts. To correct

for this possibility, we performed additional motion scrubbing (Power et al., 2012), in addition to standard motion regression during preprocessing.

Conclusion

In this study analyzing the effect of anti-epileptic medications on brain network topology of patients with TLE, we found that CBZ/OXC use is associated with a lower betweenness centrality. Our study would provide guidance for interpretation of graph-based FC studies in patients on anti-epileptic drugs. Changes in network measures should be correlated to seizure control in future studies to evaluate whether these changes play a role in the seizure-controlling properties of anti-epileptic drugs.

Acknowledgments

Dr. Haneef is funded by the Epilepsy Foundation of America Grant (Research Grants Program), the Baylor College of Medicine Computational and Integrative Biomedical Research Center (CIBR) Seed Grant Awards, and the Baylor College of Medicine Junior Faculty Seed Grant. Dr. Levin is funded by the Moody Foundation. Ms. Chiang is funded by the National Library of Medicine Training Fellowship in Biomedical Informatics, Gulf Coast Consortia for Quantitative Biomedical Sciences (Grant No. 2T15LM-007093-21) and by the National Institutes of Health (Grant No. 5T32CA096520-07).

Author Disclosure Statement

None of the authors have any competing financial interests to disclose.

References

Achard S, Bullmore E. 2007. Efficiency and cost of economical brain functional networks. PLoS Comput Biol 3:e17.

Bernhardt BC, Chen Z, He Y, Evans AC, Bernasconi N. 2011. Graph-theoretical analysis reveals disrupted small-world organization of cortical thickness correlation networks in temporal lobe epilepsy. Cereb Cortex 21:2147–2157.

Bollen KA, Jackman RW. 1990. *Modern Methods of Data Analysis*. Newbury Park, CA: Sage Publishers, pp.257–291.

Bullmore ET, Bassett DS. 2011. Brain graphs: graphical models of the human brain connectome. Annu Rev Clin Psychol 7:113–140.

Chiang S, Haneef Z. 2014. Graph theory findings in the pathophysiology of temporal lobe epilepsy. Clin Neurophysiol 125:1295–1305.

Chiang S, Stern JM, Engel J, Levin HS, Haneef Z. 2014. Differences in graph theory functional connectivity in left and right temporal lobe epilepsy. Epilepsy Res 108:1770–1781.

Fox MD, Snyder AZ, Vincent JL, Corbetta M, Van Essen DC, Raichle ME. 2005. The human brain is intrinsically organized into dynamic, anticorrelated functional networks. Proc Natl Acad Sci U S A 102:9673–9678.

Giessing C, Thiel CM. 2012. Pro-cognitive drug effects modulate functional brain network organization. Front Behav Neurosci 6:53.

Hair Jr., JF, Anderson RE, Tatham RL, Black WC. 1995. *Multivariate Data Analysis*, 3rd ed. New York: Maxwell Macmillan.

Horstmann MT, Bialonski S, Noennig N, Mai H, Prusseit J, Wellmer J, et al. 2010. State dependent properties of epileptic brain networks: comparative graph-theoretical analyses of simultaneously recorded EEG and MEG. Clin Neurophysiol 121:172–185.

Jenkinson M, Beckmann CF, Behrens TE, Woolrich MW, Smith SM. 2012. FSL. Neuroimage 62:782–790.

Jokeit H, Okujava M, Woermann FG. 2001. Carbamazepine reduces memory induced activation of mesial temporal lobe structures: a pharmacological fMRI-study. BMC Neurol 1:6.

Lammers MW, Hekster YA, Keyser A, Meinardi H, Renier WO, van Lier H. 1995. Monotherapy or polytherapy for epilepsy revisited: a quantitative assessment. Epilepsia 36:440–446.

Latora V, Marchiori M. 2001. Efficient behavior of small-world networks. Phys Rev Lett 87:198701.

Latora V, Marchiori M. 2003. Economic small-world behavior in weighted networks. Eur Phys J B 32:249–263.

Liang X, Wang J, Yan C, Shu N, Xu K, Gong G, et al. 2012. Effects of different correlation metrics and preprocessing factors on small-world brain functional networks: a resting-state functional MRI study. PLoS One 7:e32766.

Maslov S, Sneppen K. 2002. Specificity and stability in topology of protein networks. Science 296:910–913.

Pillai JJ, Williams HT, Faro S. 2007. Functional imaging in temporal lobe epilepsy. Semin Ultrasound CT MR 28:437–450.

Power JD, Barnes KA, Snyder AZ, Schlaggar BL, Petersen SE. 2012. Spurious but systematic correlations in functional connectivity MRI networks arise from subject motion. Neuroimage 59:2142–2154.

Rubinov M, Sporns O. 2010. Complex network measures of brain connectivity: uses and interpretations. Neuroimage 52:1059–1069.

Smith SM. 2002. Fast robust automated brain extraction. Hum Brain Mapp 17:143–155.

Szaflarski JP, Allendorfer JB. 2012. Topiramate and its effect on fMRI of language in patients with right or left temporal lobe epilepsy. Epilepsy Behav 24:74–80.

Tzourio-Mazoyer N, Landeau B, Papathanassiou D, Crivello F, Etard O, Delcroix N, et al. 2002. Automated anatomical labeling of activations in SPM using a macroscopic anatomical parcellation of the MNI MRI single-subject brain. Neuroimage 15:273–289.

Vaessen MJ, Jansen JF, Vlooswijk MC, Hofman PA, Majoie HJ, Aldenkamp AP, et al. 2012. White matter network abnormalities are associated with cognitive decline in chronic epilepsy. Cereb Cortex 22:2139–2147.

Vlooswijk MC, Jansen JF, Majoie HJ, Hofman PA, de Krom MC, Aldenkamp AP, et al. 2010. Functional connectivity and language impairment in cryptogenic localization-related epilepsy. Neurology 75:395–402.

Vlooswijk MC, Vaessen MJ, Jansen JF, de Krom MC, Majoie HJ, Hofman PA, et al. 2011. Loss of network efficiency associated with cognitive decline in chronic epilepsy. Neurology 77:938–944.

Wilke C, Worrell G, He B. 2011. Graph analysis of epileptogenic networks in human partial epilepsy. Epilepsia 52:84–93.

Address correspondence to:
Zulfi Haneef
Department of Neurology
Baylor College of Medicine
One Baylor Plaza, MS: NB302
Houston, TX 77030

E-mail: zulfi.haneef@bcm.edu